ACADEMIC PRESS

Available online at www.sciencedirect.com
SCIENCE DIRECT®

NeuroImage

NeuroImage 19 (2003) 271–280

www.elsevier.com/locate/ynimg

Predicting events of varying probability: uncertainty investigated by fMRI

Kirsten G. Volz,* Ricarda I. Schubotz, and D. Yves von Cramon

Max Planck Institute of Cognitive Neuroscience, Leipzig, Germany

Received 8 July 2002; accepted 30 December 2002

Abstract

Many everyday life predictions rely on the experience and memory of event frequencies, i.e., natural samplings. We used functional magnetic resonance imaging (fMRI) to investigate the neural substrates of prediction under varying uncertainty based on a natural sampling approach. The study focused particularly on a comparison with other types of externally attributed uncertainty, such as guessing, and on the frontomedian cortex, which is known to be engaged in many types of decisions under uncertainty. On the basis of preceding stimulus cues, participants predicted events that occurred with probabilities ranging from $p = 0.6$ to $p = 1.0$. In contrast to certain predictions in a control task, predictions under uncertainty elicited activations within a posterior frontomedian area (mesial BA 8) and within a set of subcortical areas which are known to subserve dopaminergic modulations. The parametric analysis revealed that activation within the mesial BA 8 significantly increased with increasing uncertainty. A comparison with other types of uncertainty indicates that frontomedian correlates of frequency-based prediction appear to be comparable with those induced in long-term stimulus-response adaptation processes such as hypothesis testing, in contrast to those engaged in short-term error processing such as guessing.

Introduction

Predictions are made on the basis of expectations about which event is the most probable to occur. Dependent on the frequency with which we experienced that an event *e* has followed the type of situation we face again, predictions are made with more or less certainty. In order to come up with a stable representation about event frequencies we must face the same type of situations over and over again, i.e., within a so-called *natural sampling* (Gigerenzer, 1994; Hasher and Zacks, 1979; Kleiter et al., 1997). The acquired representation of probabilities of an event's occurrence are applied to external stimulus properties, so that a distinction between differently probable events is possible. The high accuracy of frequency estimations observed in humans confirm the vital meaning of a correct estimation of event frequencies in many adaptive behaviors (Betsch et al., 2001; Sedlmeier, 1999).

Like guessing and gambling, probability-based predictions are charged by externally attributed uncertainty. In contrast to internally attributed types of uncertainty in decision making, externally attributed uncertainty occurs whenever we think that it is caused by events in the world that we do not control (Kahneman and Tversky, 1982; Howell and Burnett, 1978). The typical coping strategy that is used in such situations is to rate the relative frequency of such events. Brain correlates of this externally attributed uncertainty have been investigated in guessing paradigms confronting subjects with two or more events of equal probability (Elliott et al., 1999; Elliott and Dolan, 1998; Paulus et al., 2001). However, in many real life situations we do not expect one out of several events to occur with the same probability. Rather, we describe situations as indicating varying event probabilities, for instance, when saying "I am *very* certain that it will rain tomorrow" or "I am *quite* certain that Peter will be late." Hence, in contrast to predictions that we make in guessing or gambling situations, our real life predictions usually depend on extensive experi-

* Corresponding author. Max Planck Institute of Cognitive Neuroscience, P.O. Box 500 355, D-04303 Leipzig, Germany. Fax: +49-341-9940-134/221. http://www.cns.mpg.de.

E-mail address: volz@cns.mpg.de (K.G. Volz).

1053-8119/03/$ – see front matter © 2003 Elsevier Science (USA). All rights reserved.
doi:10.1016/S1053-8119(03)00122-8

ences and memories of event frequencies. Accordingly, we were interested whether activations induced by uncertainty in a natural sampling prediction would be different from or similar to those induced by uncertainty in guessing or gambling. A similarity is suggested by the fact that both types are so-called externally attributed types of uncertainty. A difference is suggested by the fact that predictions that are based on a natural sampling refer to a learning process, whereas guessing and gambling do not.

We used functional magnetic resonance imaging (fMRI) to investigate the neural correlates of predictions based on a virtual natural sampling. Participants were presented with stimulus combinations that determined the probability of a subsequently following event which occurred with a probability of $p = 0.6$, 0.7, 0.8, 0.9, or 1.0. Using a parametric design, we tested the hypothesis of whether brain activation within the region of interest, i.e., frontomedian areas, would increase with decreasing event probability. Many different tasks that require decisions or overt responses under uncertainty are known to draw on frontomedian areas (Bechara et al., 1996; Elliott et al., 1999; Elliott and Dolan, 1998; Paulus et al., 2001, 2002; Critchley et al., 2001, Rogers et al., 1999; Goel and Dolan, 2000). However, uncertainty is reported to be reflected within posterior frontomedian areas, including mesial BA 8 or anterior BA 6, corresponding to the pre-supplementary motor area (pre-SMA), and BA 24/32, i.e., the anterior cingulate cortex (ACC). Accordingly, though the engagement of frontomedian areas in behaviors under uncertainty is clearly indicated in the literature, we are ignorant about the correlates of uncertainty that we typically face in everyday behavior, i.e., natural samplings. One central aim of the present study was therefore to clarify the anatomical location within the posterior portion of the frontomedian wall that covaries positively with increasing uncertainty in prediction in a natural sampling.

In addition to posterior frontomedian areas, orbitofrontal areas are known to be engaged in uncertain decisions, particularly those induced by reward expectancy, and depending on varying task-corresponding emotional attitudes (O'Doherty et al., 2001; Rogers et al., 1999; Critchley et al., 2001; Breiter et al., 2001; Elliott et al., 1999). However, due to technical restrictions of the T2* sequence in a 3T NMR system that usually causes signal voids (Norris et al., 2002), medial orbitofrontal activations could not be detected in the present study. We therefore focus our present study on posterior frontomedian areas, including mesial BA 6, mesial BA 8, BA 32, and BA 24.

The cognitive representation of event frequencies (like "2 out of 10") are reported to differ crucially from those of event probabilities (like "20%") (Gigerenzer, 1994; Gigerenzer and Hoffrage, 1995). As we worried that strategies like coding event frequencies by event probabilities could emerge after extensive behavioral training, we decided to dismiss a training. Without a presession training, however, we expected slow learning effects during the course of the experimental session, and therewith a slow decrease of general uncertainty. As we were interested specifically in the probability-dependent uncertainty varying between blocks, we had to control for this slow learning effect. We did this by employing an additional statistical regressor that modeled learning effects (see Methods).

Methods

Participants

Sixteen right-handed, healthy volunteers (5 female, mean age 24.9, range 21–35) participated in the study. After being informed about potential risks and screened by a physician of the institution, subjects gave informed consent before participating. The experimental standards were approved by the local ethics committee of the University of Leipzig. Data were handled anonymously.

Procedure

Participants were instructed immediately before the MRI experiment. In the MRI session, subjects were supine on the scanner bed with their right and left index finger positioned on the response buttons. In order to prevent postural adjustments, the subject's arms and hands were carefully stabilized by tape. In addition, form-fitting cushions were used to prevent arm, hand, and head motion. Participants were provided with earplugs to attenuate scanner noise. Immediately prior to the functional imaging session, subjects spent 20 min in the scanner, so that they could acclimate to the confinement and sounds of the MR environment.

Stimuli and task

Stimuli consisted of pairs of pictures showing comic figures. Four different figures were employed (in the following referred to as A, B, C, and D), resulting in six possible figures combinations (A-B, A-C, A-D, B-C, B-D, and C-D). Each of the six pairings of figures was systematically associated with a particular probability, and these associations were consistent throughout the experiment. Participants were instructed to press the right or left response button corresponding to the figure they expected to win (uncertain prediction condition) or the figure that was indicated to win (control condition). Depending on the pairing in the uncertain prediction condition, the feedback showed one of two figures with a mean probability of 0.6 (that D wins against C), 0.7 (that D wins against B), 0.8 (that B wins against C), 0.9 (that C wins against A), and 1.0 (that A wins against D), respectively. One figure combination (A-B) was used as a control condition, in which concurrently presented arrows in the middle of the screen indicated which figure would win. In this condition, arrows pointed to A and to B equally often; i.e., A won against B with a probability of 0.5. Accordingly, average winning

probabilities were almost balanced between the four figures (A, 0.533; B, 0.533; C, 0.500; and D, 0.433). By balancing the probabilities in this way, we aimed to avoid cross-talk between pairings and subsequent effects like latent inhibition to operate between blocks.

We used a block presentation design, with probabilities varying between each block (0.6, 0.7, 0.8, 0.9, 1.0) and each block consisting of five subsequently presented trials of the same figure pairing (for instance, A plays five times against B). Within each trial, one pair of figures was presented for 2 s during which the participant's response was recorded.

Presentation was followed by a feedback presented for 1.5 s. In order to enhance the BOLD signal we employed a jittering that allow for assessing the BOLD response at different times relative to the event onset. We jittered both the beginning of each block and the inter-trial interval (ITI). We kept the trial duration constant at 3.5 s, and the trial onset asynchrony at 5 s. In contrast, the ITI varied, with a mean duration of 1.5 s, and a jittering of 0, 500, 1000, or 1500 ms assigned randomly to the trials.

Blocks were separated by a 5-s break. Overall, 10 blocks were presented for each of the five probabilities and the control condition, resulting in 60 blocks or 300 trials altogether. Blocks were presented in randomized order, and order was also randomized and balanced between subjects. The frequency of block-block transitions was balanced across the experimental session.

The order of blocks was balanced between subjects, such that the group-averaged event probability was 0.75 to each time during the course of the entire experimental session (see also comments on the regressor modeling slow learning effects). That is, subject 01 started, for instance, with the block order 0.7, 0.6, 1.0, and so on, whereas subject 02 started with 0.1, 0.8, 0.6, and so on. Regressor 1 (group-averaged error score for each condition) and regressor 2 (group-averaged error score for each trial) were thereby statistically independent in each subject. That is, none of the correlations were significant (two subjects $r = -0.11$, three subjects $r = 0.10$, two subjects $r = -0.17$, three subjects $r = -0.04$, three subjects $r = 0.02$, three subjects $r = 0.13$).

Imaging

Imaging was performed at 3T on a Bruker Medspec 30/100 system equipped with the standard bird-cage head coil. Slices were positioned parallel to the bicommissural plane (AC-PC) with 16 slices (thickness 5 mm, spacing 2 mm) covering the whole brain. A set of 2D anatomical images was acquired for each participant immediately prior to the functional experiment, using a MDEFT sequence (256×256 pixel matrix). Functional images in plane with the anatomical images were acquired using a single-shot gradient EPI sequence (TE = 30 ms, 64×64 pixel matrix, flip angle 90°, field of view 19.2 cm) sensitive to BOLD contrast. During each trial, 2 images were obtained from 16 axial slices at the rate of 2.5 s. In a separate session, high-resolution whole brain images were acquired from each participant to improve the localization of activation foci using a T1-weighted 3D segmented MDEFT sequence covering the whole brain.

Data analysis

The MRI data were processed using the software package LIPSIA (Lohmann et al., 2001). In the preprocessing, low-frequency signals were suppressed by applying a 1/170 Hz highpass filter. A spatial Gaussian filter with 5.65 mm FWHM was applied. The increased autocorrelation caused by the filtering was taken into account during statistical evaluation by the adjustment of the degrees of freedom. To correct for the temporal offset between the slices acquired in one image, a sinc-interpolation algorithm based on the Nyquist Shannon theorem was employed. To correct for movements, the images of the fMRI time series were geometrically aligned using a matching metric based on linear correlation. The anatomical registration was done in three steps: First, the anatomical slices geometrically aligned with the functional slices were used to compute a transformation matrix, containing rotational and translational parameters, that register the anatomical slices with the 3D reference T1-data set. In a second step, each individual transformation matrix was scaled to the standard Talairach brain size (Talairach and Tournoux, 1988) by applying a linear scaling. Finally, these normalized transformation matrices were applied to the individual functional raw data. Slice gaps were scaled using a trilinear interpolation, generating output data with a spatial resolution of $3 \times 3 \times 3$ mm (27 mm^3).

The statistical analysis was based on a least-squares estimation using the general linear model (GLM) for serially autocorrelated observations (random effects model; Friston, 1994; Worsley and Friston, 1995; Zarahn et al., 1997). The design matrix was generated with a synthetic hemodynamic response function (Friston et al., 1998; Josephs et al., 1997). The model equation, including the observation data, the design matrix, and the error term, was convolved with a Gaussian kernel of dispersion of 4 s FWHM. The model includes an estimate of temporal autocorrelation. The effective degrees of freedom were estimated as described in Worsley and Friston (1995) and in Seber (1977). In the following, contrast maps, i.e., estimates of the raw scores, were generated for each subject. As the individual functional data sets were all aligned to the same stereotactic reference space, a group analysis was subsequently performed. Groups of activated voxels were searched for ($Z > 3.09$ (Holmes and Friston, 1998) and at least 6 activated voxels) using the method of Braver et al. (2001) which also eliminates the requirement to make allowance for multiple comparisons and reduces the sensitivity to false positive activations (see also Norris et al., 2002).

Effects of prediction uncertainty were analyzed using a parametric design with two regressors (Büchel et al., 1996, 1998; Lange, 1999). In order to model the effects of pre-

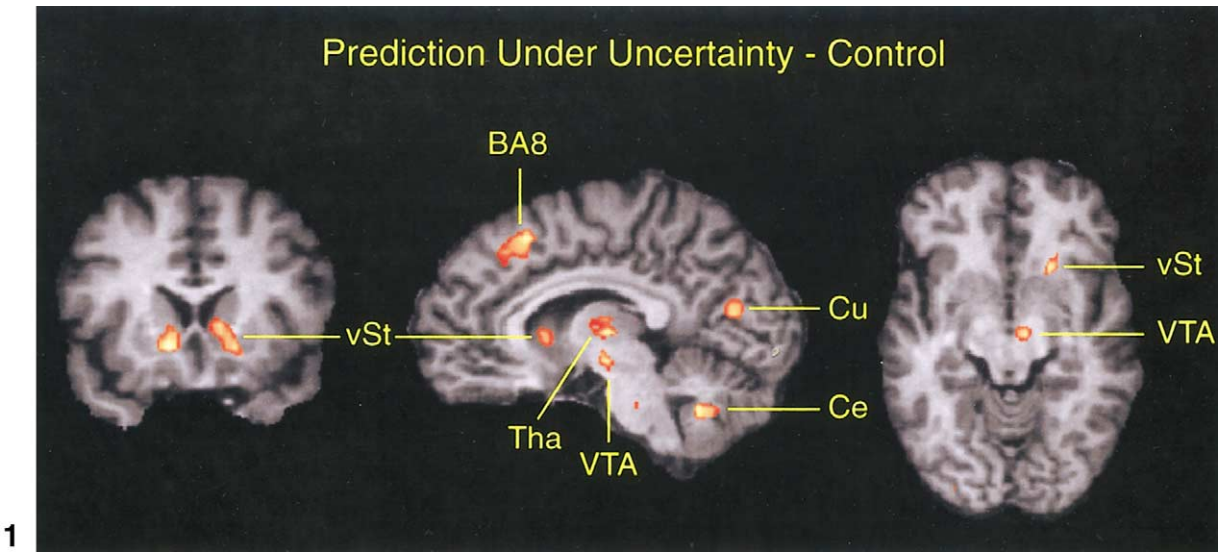

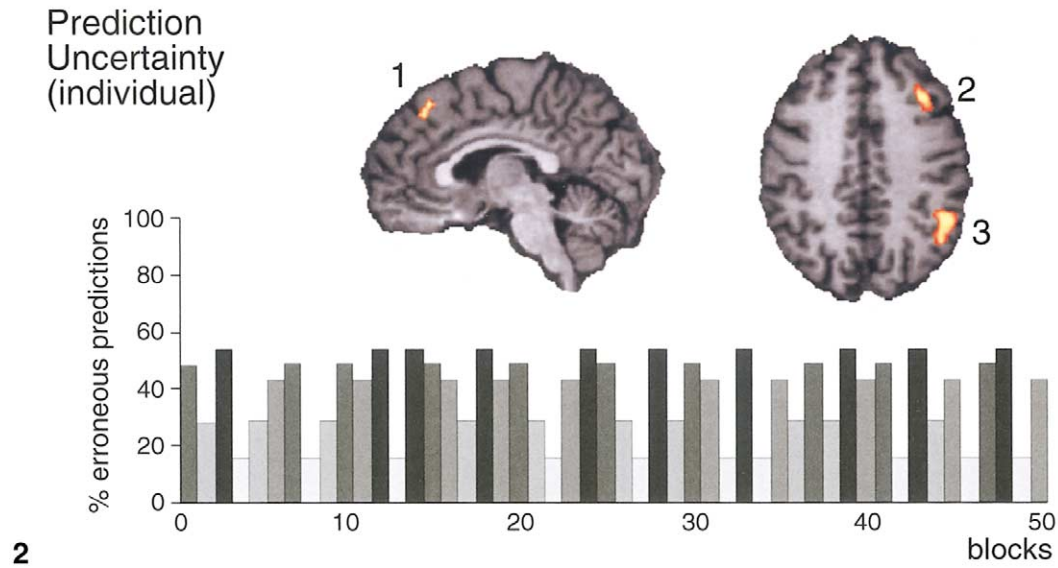

Fig. 1. Main task effect ($Z > 3.09$) for prediction under uncertainty versus control condition. Group-averaged activations are shown on coronal ($y = 12$), saggital ($x = 8$), and axial ($z = -6$) slices of an individual brain normalized and aligned to the Talairach stereotactic space. For activation coordinates, please see Table 1. Abbreviations: vST, ventral striatum; BA8, mesial Brodmann area 8; Tha, thalamus; VTA, midbrain area; Cu, cuneus, Ce, cerebellum.

Fig. 2. Parametric effects of prediction uncertainty. The upper panel shows the group-averaged activations on a saggital ($x = 4$) and an axial ($z = 36$) slice. Voxels covarying positively with prediction uncertainty were located within the mesial BA 8 (1), the middle frontal gyrus (2), and the inferior parietal lobule (3). Coordinates of further activations are given in Table 2. An example for a regressor for one subject is plotted on the lower panel. Regressors were determined individually, depending on the presentation order of blocks. The level of uncertainty was modeled by the mean prediction error made for each of the five probabilities. Bars for each experimental block are shown in different intensities of gray. Note that the 10 blocks of control condition did not enter the parametric analysis and are therefore not shown in the figure.

diction uncertainty as measured by performance, a regressor was used which consisted of the average prediction error per probability of event occurrence, i.e., the group-averaged error score for each of the five experimental conditions (regressor 1). Within the same model, we tested for slow learning effects by using a second regressor, consisting of the group-averaged error score for each experimental trial (regressor 2). Note that such a second regressor can only be useful if it models a different source of variance than the first regressor, i.e., block-dependent uncertainty. As learning effects were expected to depend on block-wise probabilities of event occurrence, we employed a group-related regressor for learning effects. This group-averaged learning effect was statistically independent from the block-wise variation of uncertainty. This was achieved by balancing the order of event probabilities between subjects, such that the group-averaged event probability was the same for each time during the course of the entire experimental session (see also stimuli and task section). Both regressors referred to the same sample of trials, including all uncertain predic-

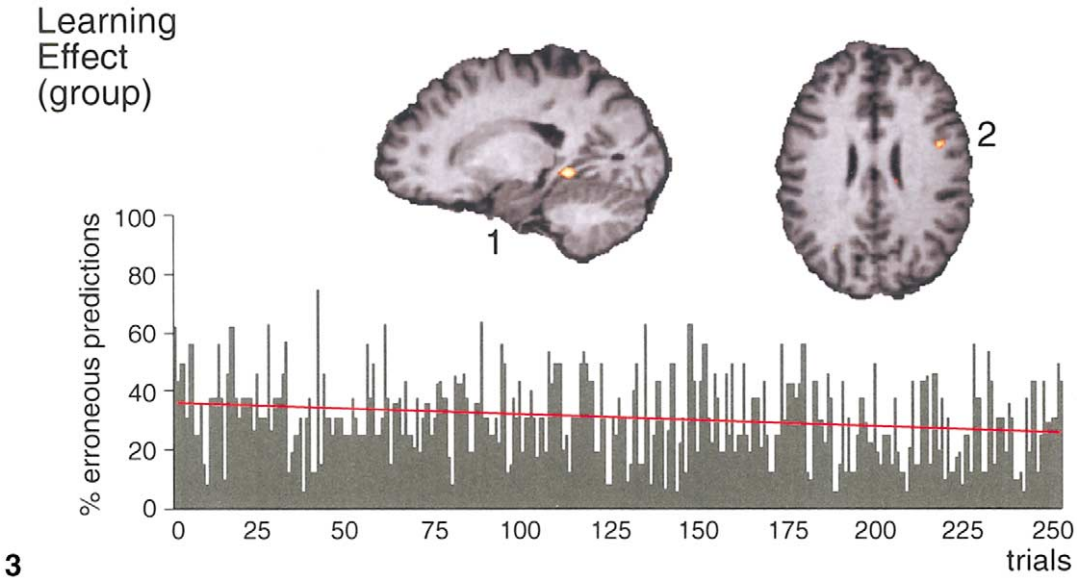

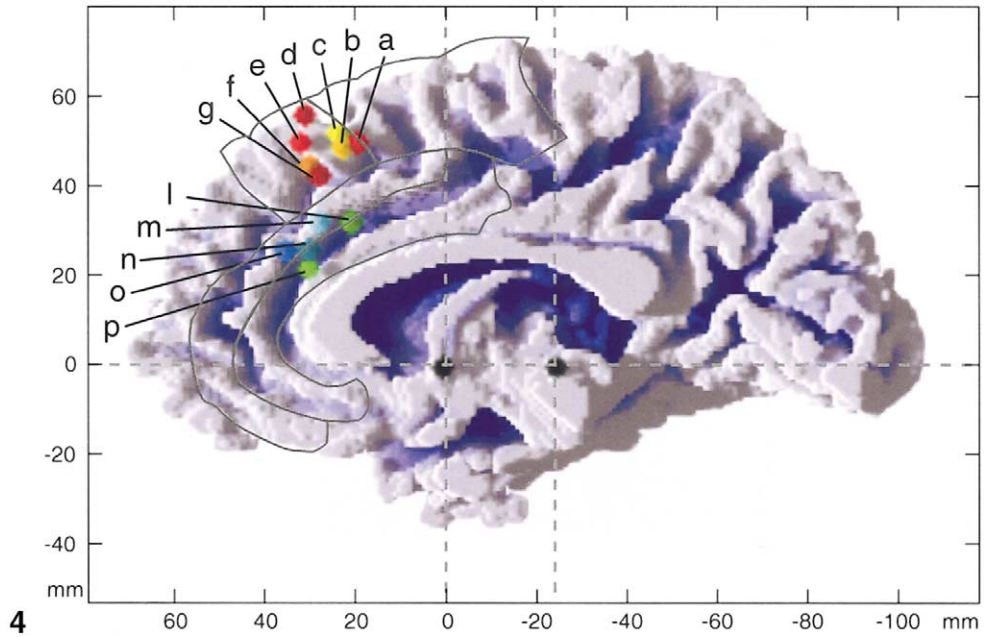

Fig. 3. Parametric effects of learning. The upper panel shows the group-averaged activations on a left saggital slice ($x = 43$) and an axial slice ($z = 3$). Voxels covarying positively with the decreasing error rates in the course of the experimental session were found within the left posterior parahippocampal gyrus (1) ($x = -18$, $y = -44$, $z = -3$; $Z = 4.1$) and within the right inferior frontal junction area (2) ($x = 43$, $y = 0$, $z = 26$; $Z = 3.5$). The lower panel shows the regressor that modeled decreasing uncertainty due to slow learning effects across subjects (gray bars). The regressor based on the group-averaged mean prediction error for each trial of the experimental condition (5 trials per block, 50 blocks = 250 trials). The red line indicates the linear learning trend, showing that erroneous predictions decreased from about 36% at the beginning to 28% at the end of the session (expected maximal performance was 25%). As in Fig. 2, the 50 trials of control condition are not plotted as they did not enter the parametric analysis.

Fig. 4. Comparison between frontomedian activations of the present study (a, e) and those of other studies on decisions under uncertainty. The right fronomedian wall of a white matter segmented individual brain is shown from the midline. The outer frame shows coordinates from Talairach and Tournoux (1988). Crosshairs cut through the anterior and the posterior commissure (AC-PC), with vertical orientation lines (VAC-VPC) perpendicular to AC-PC, respectively. Brodmann areas 6, 8, 24, and 32 are outlined. Red-yellow spheres refer to activation foci within mesial BA 8, green-blue spheres to those within BA 24/32. The red sphere a corresponds to the main task effect of prediction under uncertainty, compared to the control condition (see also Fig. 1). The sphere e corresponds to the parametric effect of increasing prediction uncertainty (see also Fig. 2). Other letters and spheres correspond to the following studies; b, Schubotz and von Cramon, 2002 (prediction difficulty); c, Elliott and Dolan, 1998 (hypothesis testing); d and g, Goel and Dolan, 2000 (rule application); f, Ullsperger and von Cramon, 2001 (response competition); I, Ullsperger and von Cramon, 2001 (error detection); m, Elliott and Dolan, 1998 (committing oneself to choice); n, Critchley et al., 2001 (uncertainty and arousal); o, Elliott et al., 1999 (guessing); p, Rogers et al., 1999 (risky choice).

Table 1
Anatomical specification, hemisphere, Talairach coordinates (*x*, *y*, *z*), and maximal *Z*-scores (*Z*) of significantly activated voxels in prediction under uncertainty (all levels collapsed) in contrast to prediction under certainty (control condition)

Area	Hemisphere	*x*	*y*	*z*	*Z*
Frontomedian cortex (BA 8/6)	R	8	18	46	4.4
Ventral striatum	L	−12	12	−3	4.5
	R	21	15	−6	4.0
Thalamus	L	−15	−18	12	3.4
	R	8	−17	6	4.2
Midbrain area	R	8	−17	−6	3.9
Anterior insula	R	40	19	6	4.1
Cerebellum	R	1	−68	−23	4.7
Cuneus	R	4	−71	14	4.1

tion conditions, but excluding the control condition. The control condition was modeled as a separate onset vector within the same model. By including both regressors within one statistical model, contrast maps could be generated that extracted the three effects of interest independently from each other. Three contrast maps were generated from that statistical model. In the first, all uncertain prediction blocks were collapsed and contrasted against certain prediction, i.e., the control condition. Thereby, we tested for the main task effect only. In the second contrast, the effects of probability-dependent uncertainty in prediction were tested using regressor 1. In the third contrast, the effects of time-dependent uncertainty were tested using regressor 2. Note that regressor 1, which was different for each subject according to the order of blocks, and regressor 2, which was the same for each subject, modeled statistically independent sources of variance and did not correlate.

Results

Behavioral data

Performance was measured by the rate of erroneous predictions and reaction times of correct predictions. A repeated-measures ANOVA with the 6-level factor *uncertainty* (P = 0.6, 0.7, 0.8, 0.9, 1.0, and control) yielded a significant main effect for both erroneous predictions ($F(5,75) = 110.8$, $P < 0.0001$) and reaction times ($F(5,75) = 6.93$, $P < 0.001$). Main effects were also significant when the control condition did not enter the ANOVA (erroneous predictions $F(4,60) = 54.5$, $P < 0.0001$; reaction times $F(4,60) = 5.95$, $P < .001$). A two-sided Pearson correlation between erroneous predictions and time was found to be significantly negative ($r = -0.19$; $P < 0.001$). Accordingly, the explained variance of the slow learning effect was 1.69%. Likewise, reaction times got significantly shorter in the course of the experiment, as indicated by a significantly negative two-sided Pearson correlation ($r = -0.43$; $P < 0.0001$). Together, decreasing rates of both erroneous predictions and reaction times indicated significant slow learning effects over time.

FMRI data

In order to test for the main task effect in a first step, we collapsed all levels of prediction under uncertainty and contrasted them together against the control condition. As listed in Table 1 and shown in Fig. 1, significant activations were elicited within right frontomedian cortex (mesial BA 8/6), the right anterior insula, the cuneus, the cerebellar vermis extending laterally into the paramedian portion of the left cerebellar hemisphere, and within a subcortical network, including the ventral striatum, the thalamus, and the right midbrain area (VTA).

When testing for the parametric effects of prediction uncertainty, we found positively covarying voxels to be located within the right posterior frontomedian cortex (mesial BA 8), the right thalamus, the right anterior insula, and the left cerebellar cortex (Table 2 and Fig. 2). Hence, the right mesial BA 8 was the only cortical area that was found to be activated both in contrast to the control condition (main task effect) and in the parametric modulation of probability-dependent prediction uncertainty (parametric effect). Some areas that were activated significantly in the main task effect did not covary positively with increasing uncertainty. Additional activations were located within the right middle frontal gyrus and superior frontal sulcus, and the midportion of the right intraparietal sulcus. Though these areas were also slightly activated in the main task effect, maximal *Z*-scores remained below the statistical threshold.

Finally, we tested for voxels that covaried positively with decreasing uncertainty due to slow learning effects in the course of the experimental session (Fig. 3). As a result, we found significant activation within only two areas, one located at the junction of the right inferior precentral sulcus and the right inferior frontal sulcus (inferior frontal junction area, IFJ), the other within the left posterior parahippocampal gyrus. Hence, there was no area that was commonly activated by probability-dependent uncertainty in prediction and by decreasing uncertainty due to slow learning effects.

Table 2
Anatomical specification, hemisphere, Talairach coordinates (*x*, *y*, *z*), and maximal *Z*-scores (*Z*) of voxels covarying positively with increasing prediction uncertainty

Area	Hemisphere	*x*	*y*	*z*	*Z*
Frontomedian cortex (BA 8)	R	4	30	46	3.9
Thalamus	R	8	−11	9	3.4
Anterior insula	R	37	12	−3	3.6
Cerebellum	L	−18	−71	−29	4.0
Superior frontal sulcus	R	17	3	46	3.6
Middle frontal gyrus	R	37	21	36	3.7
Inferior parietal lobule	R	46	−53	38	4.0

Discussion

The present fMRI study investigated brain areas particularly within the frontomedian cortex that covary positively with a parametric modulation of prediction uncertainty in a virtual natural sampling approach. To that end, different degrees of prediction uncertainty were induced by different probabilities of event occurrence. In contrast to a control condition that allowed a certain prediction on the basis of external cues, prediction under uncertainty engaged the mesial BA 8. Though the maximally activated voxel of the frontomedian activation was located on the border between BA 6 and BA 8, closer inspection revealed that voxels activated above the statistical threshold were only found anteriorly to the activation maximum, that is, within BA 8, but not within BA 6. This was further supported by the parametric analysis. When testing for voxels that covary positively with increasing uncertainty in prediction as measured by the mean prediction error across blocks, we found activation to be clearly located within mesial BA 8.

In contrast to the control condition, prediction under uncertainty induced also activation within a sample of subcortical areas, including several foci within the midbrain (ventral tegmental area, VTA), the ventral striatum (nc. accumbens), and the dorsal thalamus. These structures belong to a striatal-thalamo-cortical network basically prominent in reward-based learning functions (Graybiel, 2000; Breiter et al., 2001; Delgado et al., 2000; Elliott et al., 2000). As in the currently employed natural sampling approach, such types of learning are typically characterized by a slow delayed acquisition rate of implicit stimulus-response associations. In particular, the nc. accumbens is taken to support the ability to work for delayed rewards (Cardinal et al., 2002). It is suggested that erroneous predictions function as a "teaching signal" for phasic changes in dopaminergic activity (Hollerman and Schultz, 1998; Schultz and Dickinson, 2000; Schultz, 1998). Thereby, dopaminergic projections from the VTA through the ventral striatum and the frontomedian cortex (Williams and Goldman-Rakic, 1998) provide phasic signals to modify and update stimulus-response mappings (Inase et al., 1999). Activations that we found within these areas can be reconciled with the idea of a summative, value-based attitude formation in natural samplings (Betsch et al., 2001). This approach assumes that, in natural samplings, the responses evoked by perceptual events are automatically recorded and summed up. Subsequently, these summary evaluations can serve as a basis for predictions and corresponding behavioral responses.

However, it must also be considered that uncertainty was not the only aspect to vary between conditions. Rather, the expectancy and the experience of positive and negative prediction outcome varied too. Since a positive prediction outcome could be seen as a kind of reward, a related issue here is whether expectancy and experience of reward can be dissociated on the brain level. Recent imaging studies have indicated that expectancy and previous experience mostly share common neural substrates (Breiter et al., 2001), as already suggested by the work of Mellers and colleagues (1997, 1999). Accordingly, the frontomedian areas found to be activated in the present study could be differently modulated by either the expectancy or the experience of positive prediction outcomes.

Increasing uncertainty reflected within mesial BA 8

Uncertain versus certain prediction elicited activation within mesial BA 8. The maximally activated voxel was located at the border to mesial BA 6, i.e., the pre-SMA, whereas the parametric effect of increasing uncertainty induced maximal activation anteriorly within mesial BA 8. Though this outcome raises the question of functional differences and similarities between anterior mesial BA 6/pre-SMA and mesial BA 8, these are difficult to determine in the literature. On the one hand, the pre-SMA role in higher movement organization is long established, in contrast to hierarchically lower movement output organization attributed to the posteriorly adjacent SMA proper (Picard and Strick, 1996, 2001; Shima and Tanji, 1998). Specifically, the pre-SMA receives converging and rich input from all lateral prefrontal areas, which in turn are target regions from sensory cortices (Bates and Goldman-Rakic, 1993; Luppino et al., 1993). The pre-SMA is therefore suggested in "cognitive" rather than motor aspects of voluntary behavior, particularly in the anticipatory processing of sensory (visual) information in view of a potential decision making or motor selection (Ikeda et al., 1999; Picard and Stick, 2001). On the other hand and in contrast to the pre-SMA, less is known about the functional profile of the anteriorly adjacent mesial BA 8. Projections between the monkey homologue of the pre-SMA, area F6 (Matelli et al., 1985), and anteriorly adjacent areas of the frontomedian wall suggest a close functional relationship (Luppino et al., 1993). Tracer studies in the monkey do not explicitly differentiate between mesial BA 6 and adjacent 8, but in contrast point out that rich prefrontal projections target the rostral SMA so anteriorly that this target area may include Walker's medial area 8b (Bates and Goldman-Rakic, 1993). In accordance with frontoparietal projections investigated in the monkey, we found right frontal and parietal areas together with mesial 8 to be increasingly activated by increasing prediction uncertainty.

Also in imaging studies, mesial BA 8 and pre-SMA are often reported to be engaged in the same task and contrast. For instance, mesial BA 8 and preSMA together show increased activation whenever conflicts arise about the correspondence between perceived events and appropriate motor selections (Ullsperger and von Cramon, 2001). Likewise, predicting serial events in increasingly complex stimulus trains increased pre-SMA activation near the border or even including a portion of mesial BA 8 (Schubotz and von Cramon, 2002). More clearly separated from BA 6 are functions of the mesial BA 8 in hypothesis testing

(Elliott and Dolan, 1998) and rule application (Goel and Dolan, 2000). Elliott and Dolan discuss mesial BA 8 activation in terms of a response selection guided by mnemonic representations of adaptive stimulus-response mappings, rather than by internally guided guessing. Similarly, Goel and Dolan refer to the anticipatory functions of BA 8, suggesting that subjects anticipate stimuli in view of activated response rules for these stimuli. Note, however, that these authors refer to mesial BA 8 as pre-SMA. Indirect evidence for a functional difference between mesial BA 8 and pre-SMA may come from findings that indicate the pre-SMA do not covary with the amount of errors made in a visuo-manual learning paradigm (Sakai et al., 1999). In contrast, mesial BA 8 activation was found to covary with errors in our study. A cautious suggestion may therefore be that BA 6 (pre-SMA) and mesial BA 8 are both involved in the acquisition of stimulus-response associations, with the latter to modulate this learning process by error evaluation.

Uncertain predictions based on natural samplings in contrast to other types of decisions under uncertainty

The aim of the present study was to figure out whether prediction based on a natural sampling induces similar or different frontomedian activations as other externally attributed types of uncertainty, particularly guessing or gambling. When comparing activations from the present study with those of other types of uncertainty-inducing tasks, two different activation clusters emerge. As plotted in Figure 4, activations reported in guessing paradigms (Elliott et al., 1999), error detection (Ullsperger and von Cramon, 2001), and risky choice (Rogers et al., 1999; Crtichley et al., 2001) elicited activations within BA 24/32. In contrast, we found our activations to be located similarly as those of hypothesis testing (Elliott and Dolan, 1998), response competition (Ullsperger and von Cramon, 2001), rule application (Goel and Dolan, 2000), and sequence-based stimulus prediction (Schubotz and von Cramon, 2002), i.e., within mesial BA 8 and 6.

This comparison indicates that activations induced by uncertainty in a natural sampling prediction are indeed different from those induced by uncertainty in guessing, although both types are so-called externally attributed types of uncertainty. As suggested in the introduction, differences in frontomedian correlates may instead reflect that predictions based on a natural sampling refer to a learning process and memory, whereas guessing and gambling do not. In comparison to further activations induced by decision under uncertainty, a common characteristic of tasks that elicit similar activations like our natural sampling approach may be that uncertainty is reduced in the long run. They involve the setting up of a model that is tested and that helps us to adapt our behavior stepwise and in a cumulative manner. In contrast, guessing and risky choices involve a short-term error processing, but no long-term behavioral adaptation to valid stimulus-response rules. Accordingly, the main difference between tasks activating BA 24/32 and those activating BA 8/6 may be that the former do not allow for learning and adaptation processes, but function more as an alerting system. This difference may include also emotional processes, which should have higher impact on fast behavioral adaptations rather than on long-lasting learning. Accordingly, BA 24/32 is suggested in the integration of cognitive processing of uncertainty with corresponding adaptive changes in bodily states (Critchley et al., 2001) or evaluative processes related to the emotional consequences of a (risky) choice (Elliott and Dolan, 1998).

Together with results discussed in the literature, we take our findings to indicate that the mesial BA 8 is particularly engaged in feedback-based testing models or hypothesis on valid stimulus-response associations that lead to long-lasting behavioral modifications. In contrast, BA 24/32 appears rather to be engaged in the fast correction of response errors, including or modulated by a short-term emotional evaluation.

Decreasing uncertainty by slow learning effects over the course of the experimental session

We expected learning effects during the course of the experiment to decrease uncertainty related to knowledge. We controlled for learning effects by modeling a second regressor using the group-averaged error score for each trial. In addition, however, we also looked directly for the effects of regressor 2 in order to confirm nonoverlapping brain activations for slow learning and frequency-dependent uncertainty. As a result, significant activations were found only within two regions, the right IFJ and the posterior parahippocampal gyrus. Activations within the posterior frontolateral cortex have been reported in a shifting cognitive set, i.e., the switching from one response tendency based on previous experiences to a currently more suitable one (Brass and von Cramon, 2002; Konishi et al., 1999; Monchi et al., 2001; Nakahara, 2002). According to this view, a decline in IFJ activation would reflect decreasing requirements on switching between different stimulus-response associations. With increasing familiarity with the stimulus pairings and their probabilistic meaning, the requirements on behavioral switching and flexibility may decline during the course of the experimental session. This would also apply to decreasing activation within parahippocampal sites, which show slow sustained modulations during new stimulus-response learning (Cahusac et al., 1993). However, the crucial implication of this finding is that slow learning effects and the reduction of prediction uncertainty draw on different, nonoverlapping brain areas, so that learning effects did not distort the activation pattern we were interested in.

Acknowledgments

We thank Markus Ullsperger for helpful comments on the manuscript, Karsten Müller, André Szameitat, and Stefan Zysset for support in fMRI statistics, and Andrea Gast-Sandmann for the stimulus material. This work was supported by the German Research Foundation (SPP 1107).

References

Bates, J.F., Goldman-Rakic, P.S., 1993. Prefrontal connections of medial motor areas in the rhesus monkey. J. Comp. Neurol. 336, 211–228.

Bechara, A., Tranel, D., Damasio, H., and Damasio, A.R., 1996. Cereb. Cortex 6, 215–225.

Betsch, T., Plessner, H., Schwieren, C., Gütig, R., 2001. I like it but I don't know why: a value-account approach to implicit attitude formation. Pers. Soc. Psychol. Bull. 27, 242–253.

Brass, M., von Cramon, Y.D., 2002. The role of the frontal cortex in task preparation. Cereb. Cortex 12, 908–914.

Braver, T.S., Barch, D.M., Kelley, W.M., Buckner, R.L., Cohen, N.J., Miezin, F.M., Snyder, A.Z., Ollinger, J.M., Akbudak, E., Conture, T.E., Petersen, S.E., 2001. Direct comparison of prefrontal cortex regions engaged in working memory and long-term memory tasks. NeuroImage 14, 48–59.

Breiter, H.C., Aharon, I., Kahneman, D., Dale, A., 2001. Functional Imaging of neural responses to expectancy and experiences of monetary gains and losses. Neuron 30, 619–639.

Büchel, C., Holmes, A.P., Rees, G., Friston, K.J., 1998. Characterizing stimulus-response functions using nonlinear regressors in parametric fMRI experiments. NeuroImage 8, 140–148.

Büchel, C., Wise, R.J.S., Mummery, C.J., Poline, J.-B., Friston, K.J., 1996. Nonlinear regression in parametric activation studies. NeuroImage 4, 60–66.

Cahusac, P.M., Rolls, E.T., Miyashita, Y., Niki, H., 1993. Modification of the responses of hippocampal neurons in the monkey during the learning of a conditional spatial response task. Hippocampus 3, 29–42.

Cardinal, R.N., Parkinson, J.A., Hall, J., Everitt, B.J., 2002. Emotion and motivation: the role of amygdala, ventral striatum, and prefrontal cortex. Neurosci. Biobehav. Rev. 26, 321–351.

Critchley, H.D., Mathias, C.J., Dolan, R.J., 2001. Neural activity in the human brain relating to uncertainty and arousal during anticipation. Neuron 29, 537–545.

Delgado, M.R., Nystrom, L.E., Fissell, C., Noll, D.C., Fiez, J.A., 2000. Tracking the hemodynamic responses to reward and punishment in the striatum. J. Neurophysiol. 84, 3072–3077.

Elliott, R., Dolan, R.J., 1998. Activation of different anterior cingulate foci in association with hypothesis testing and response selection. NeuroImage 8, 17–29.

Elliott, R., Friston, K.J., Dolan, R.J., 2000. Dissociable neural responses in human reward systems. J. Neurosci. 20, 6159–6165.

Elliott, R., Rees, G., Dolan, R.J., 1999. Ventromedial prefrontal cortex mediates guessing. Neuropsychologia 37, 403–411.

Friston, K.J., 1994. Statistical parametric mapping, in: Thatcher, R.W., Hallet, M., Zeffiro, T., John, E.R., Huerta, M. (Eds.), Functional Neuroimaging. Academic Press, San Diego, pp. 79–93.

Friston, K.J., Fletcher, P., Josephs, O., Holmes, A., Rugg, M.D., Turner, R., 1998. Event-related fMRI: characterizing differential responses. NeuroImage 7, 30–40.

Gigerenzer, G., 1994. Why the distinction between single-event probabilities and frequencies is important for psychology (and vice versa), in: Wright, G., Ayton, P. (Eds.), Subjective Probability. Wiley, Chichester, pp. 129–161.

Gigerenzer, G., Hoffrage, U., 1995. How to improve Bayesian reasoning without instruction: frequency formats. Psychol. Rev. 102, 684–704.

Goel, V., Dolan, R.J., 2000. Anatomical segregation of component processes in an inductive inference task. J. Cogn. Neurosci. 12, 110–119.

Graybiel, A.M., 2000. The basal ganglia. Curr. Biol. 10, R509–R511.

Hasher, L., Zacks, R.T., 1979. Automatic and effortful processes in memory. J. Exp. Psychol.Gen. 108, 356–388.

Hollermann, J.R., Schultz, W., 1998. Dopamine neurons report an error in the temporal prediction of reward during learning. Nature Neurosci. 1, 304–309.

Holmes, A.P., Friston, K.J., 1998. Generalisability, random effects and population inference. NeuroImage 7, 754.

Howell, M.J., Burnett, S.A., 1978. Uncertainty measurement: a cognitive taxonomy. Org. Behav. Hum. Perform. 22, 45–68.

Ikeda, A., Yazawa, S., Kunieda, T., Ohara, S., Terada, K., Mikuni, N., Nagamine, T., Taki, W., Kimura, J., Shibasaki, H., 1999. Cognitive motor control in human presupplementary motor area studied by subdural recordings of discrimination/selection-related potentials. Brain 122, 915–931.

Inase, M., Tokuno, H., Nambu, A., Akazawa, T., Takada, M., 1999. Corticostriatal and corticosubthalamic input zones from the presupplementary motor area in the macaque monkey: comparison with the input zones from the supplementary motor area. Brain Res. 833, 191–201.

Josephs, O., Turner, R., Friston, K.J., 1997. Event-related fMRI. Hum. Brain Mapp. 5, 243–248.

Kahneman, D., Tversky, A., 1982. Variants of uncertainty. Cognition 11, 143–157.

Kleiter, G.D., Krebs, M., Doherty, M.E., Garavan, H., Chadwick, R., Brake, G., 1997. Do subjects understand base rates? Organ. Behav. Hum. Decis. Process. 72, 25–61.

Konishi, S., Kawazu, M., Uchida, I., Kikyo, H., Asakura, I., Miyashita, Y., 1999. Contribution of working memory to transient activation in human inferior prefrontal cortex during performance of the Wisconsin Card Sorting Test. Cereb. Cortex 9, 745–753.

Lange, N., 1999. Statistical procedures for functional MRI, in: Moonen, C.T.W., Bandettini, P.A. (Eds.), Functional MRI. Springer, Heidelberg, pp. 301–335.

Lohmann, G., Mueller, K., Bosch, V., Mentzel, H., Hessler, S., Chen, L., Zysset, S., von Cramon, D.Y., 2001. LIPSIA—a new software system for the evaluation of functional magnetic resonance images of the human brain. Comput. Med. Imaging Graph. 25, 449–457.

Luppino, G., Matelli, M., Camarda, R., Rizzolatti, G., 1993. Corticocortical connections of area F3 (SMA-proper) and area F6 (pre-SMA) in the macaque monkey. J. Comp. Neurol. 338, 114–1140.

Matelli, M., Luppino, G., Rizzolatti, G., 1985. Patterns of cytochrome oxidase activity in the frontal agranular cortex of the macaque monkey. Behav. Brain Res. 18, 125–136.

Mellers, B., Schwartz, A., Ritov, I., 1999. Emotion-based choice. J. Exp. Psychol. Gen. 128, 332–345.

Mellers, B., Schwartz, A., Ho, K., Ritov, I., 1997. Decision affect theory: emotional reactions to the outcomes of risky options. Psychol. Sci. 8, 423–429.

Monchi, O., Petrides, M., Petre, V., Worsley, K., Dagher, A., 2001. Wisconsin Card Sorting revisited: distinct neural circuits participating in different stages of the task identified by event-related functional magnetic resonance imaging. J. Neurosci. 21, 7733–7741.

Nakahara, K., Hayashi, T., Konishi, S., Miyashita, Y., 2002. Functional MRI of macaque monkeys performing a cognitive set-shifting task. Science 295, 1532–1536.

Norris, D.G., Zysset, S., Mildner, T., Wiggins, C.J., 2002. An investigation of the value of spin-echo-based fMRI using a Stroop color-word matching task and EPI at 3T. NeuroImage 15, 719–726.

O'Doherty, J.O., Kringelbach, M.L., Rolls, E.T., Hornak, J., Andrews, C., 2001. Abstract reward and punishment representations in the human orbitofrontal cortex. Nature Neurosci. 4, 95–102.

Paulus, M.P., Hozack, N., Frank, L., Brown, G.G., 2002. Error rate and outcome predictability affect neural activation in prefrontal cortex and anterior cingulate during decision making. NeuroImage 15, 836–846.

Paulus, M.P., Hozack, N., Zauscher, B., McDowell, J.E., Frank, L., Brown, G.G., Braff, D.L., 2001. Prefrontal, parietal, and temporal cortex networks underlie decision-making in the presence of uncertainty. NeuroImage 13, 91–100.

Picard, N., Strick, P.L., 2001. Imaging the premotor areas. Curr. Opin. Neurobiol. 11, 663–672.

Picard, N., Strick, P.L., 1996. Motor areas of the medial wall: a review of their location and functional activation. Cereb. Cortex 6, 342–353.

Rogers, R.D., Owen, A.M., Middelton, H.C., Williams, E.J., Pickard, J.D., Sahakian, B.J., Robbins, T.W., 1999. Choosing between small, likely rewards and large, unlikely rewards activates inferior and orbital prefrontal cortex. J. Neurosci. 20, 9029–9038.

Sakai, K., Hikosaka, O., Miyauchi, S., Sasaki, Y., Fujimaki, N., Puetz, B., 1999. Presupplementary motor area activation during sequence learning reflects visuo-motor association. J. Neurosci. 19, RC1.

Schubotz, R.I., von Cramon, D.Y., 2002. A blueprint for target motion: fMRI reveals perceptual complexity to modulate a premotor-parietal network. NeuroImage 16, 920–935.

Schultz, W., 1998. Predictive reward signal of dopamine neurons. J. Neurophysiol. 80, 1–27.

Schultz, W., Dickinson, A., 2000. Neuronal coding of prediction errors. Annu. Rev. Neurosci. 23, 473–500.

Seber, G.A.F., 1977. Linear Regression Analysis. Wiley, New York.

Sedlmeier, P., 1999. L Erlbaum, Mahwah, NJ.

Shima, K., Tanji, J., 1998. Both supplementary and presupplementary motor areas are crucial for the temporal organization of multiple movements. J. Neurophysiol. 80, 3247–3260.

Talairach, P., Tournoux, J., 1988. Thieme, Stuttgart.

Ullsperger, M., von Cramon, D.Y., 2001. Subprocesses of performance monitoring: a dissociation of error processing and response competition revealed by event-related fMRI and ERP's. NeuroImage 14, 1387–1401.

Williams, S.M., Goldman-Rakic, P.S., 1998. Widespread origin of the primate mesofrontal dopamine system. Cereb. Cortex 8, 321–345.

Worsley, K.J., Friston, K.J., 1995. Analysis of fMRI time-series revisited — again. NeuroImage 2, 173–181.

Zarahn, E., Aguirre, G.K., D'Esposito, M., 1997. Empirical analyses of BOLD fMRI statistics. NeuroImage 5, 179–197.